




Immune predictors of response to immune checkpoint inhibitors in mismatch repair-deficient endometrial cancer

Juan Francisco Grau Bejar ^{1,2}, Elisa Yaniz Galende,² Qinghe Zeng,^{3,4} Catherine Genestie,⁵ Etienne Rouleau,⁶ Marco de Bruyn ⁷, Christophe Klein,⁴ Audrey Le Formal,² Elodie Edmond,⁸ Maëva Moreau,⁶ Annechien Plat,⁷ Sebastien Gouy,⁹ Amandine Maulard,⁹ Patricia Pautier,¹⁰ Judith Michels,¹⁰ Ana Oaknin ¹, Emeline Colomba-Blameble,¹⁰ Alexandra Leary^{2,10}

To cite: Grau Bejar JF, Yaniz Galende E, Zeng Q, *et al.* Immune predictors of response to immune checkpoint inhibitors in mismatch repair-deficient endometrial cancer. *Journal for ImmunoTherapy of Cancer* 2024;**12**:e009143. doi:10.1136/jitc-2024-009143

► Additional supplemental material is published online only. To view, please visit the journal online (<https://doi.org/10.1136/jitc-2024-009143>).

Accepted 04 June 2024

ABSTRACT

Background Patients with mismatch repair-deficient (MMRd) endometrial cancer (EC) can derive great benefit from immune checkpoint inhibitors (ICI). However not all responses and predictors of primary resistance are lacking.

Methods We compared the immune tumor microenvironment of MMRd EC ICI-responders (Rs) and ICI non-responders (NRs), using spatial multiplexed immune profiling and unsupervised hierarchical clustering analysis.

Results Overall, NRs exhibited drastically lower CD8⁺, absent terminally differentiated T cells, lack of mature tertiary lymphoid structures and dendritic cells, as well as loss of human leukocyte antigen class I. However, no single marker could predict R versus NR with confidence. Clustering analysis identified a combination of four immune features that demonstrated that accurately predicted ICI response, with a discriminative power of 92%. Finally, 80% of NRs lacked programmed death-ligand 1, however, 60% exhibited another actionable immune checkpoint (T-cell immunoglobulin and mucin containing protein-3, indoleamine 2,3-dioxygenase 1, or lymphocyte activation gene 3).

Conclusions These findings underscore the potential of immune tumor microenvironment features for identifying patients with MMRd EC and primary resistance to ICI who should be oriented towards trials testing novel immunotherapeutic combinations.

INTRODUCTION

Endometrial cancer (EC) represents the sixth most frequently diagnosed cancer in women, with an incidence of 4.5% and 417,000 new cases in 2020, mainly in developed countries.¹ Over the last 20 years, its incidence and mortality have steadily increased by about 1% per year among postmenopausal women.² Although early-stage disease is associated with an excellent prognosis, patients with advanced or recurrent disease have poor survival outcomes, with a 5-year overall survival (OS) rate of 20–25%. Until

WHAT IS ALREADY KNOWN ON THIS TOPIC

⇒ Currently, mismatch repair-deficient (MMRd) and tumor mutation burden-high status are considered the most robust predictive biomarkers of response to immune checkpoint inhibitors in endometrial cancer (EC), however only half of these patients draw a significant clinical benefit from immunotherapy.

WHAT THIS STUDY ADDS

⇒ Our study represents the first comprehensive comparison of the immune tumor microenvironment between immune checkpoint inhibitor (ICI)-responders and non-responders within an advanced or recurrent MMRd EC population. By delving into this unexplored area, our study provides insights into novel predictive biomarkers of response to ICI tailored to the distinctive immune characteristics of MMRd EC. Our research uncovered a set of four immune markers that predicted ICI response with a discriminative power of 92%, surpassing the accuracy of conventional biomarkers.

HOW THIS STUDY MIGHT AFFECT RESEARCH, PRACTICE OR POLICY

⇒ Our findings enable more precise patient selection and better prediction of primary resistance to ICIs in the MMRd EC population. This insight may help to stratify patients in future clinical trials for exploring alternative therapeutic strategies beyond anti-programmed death-ligand 1 monotherapies. Moreover, our data hold potential applicability to other MMRd cancers, such as colorectal cancer. The use of immunohistochemical techniques on archived formalin-fixed paraffin-embedded tumor blocks, cost-effective and easily applicable in clinical settings, enhances the reproducibility and accessibility of our findings.

recently, treatment options for patients progressing during or after platinum were limited and not very effective.³ In recent years, novel therapies have been



© Author(s) (or their employer(s)) 2024. Re-use permitted under CC BY-NC. No commercial re-use. See rights and permissions. Published by BMJ.

For numbered affiliations see end of article.

Correspondence to

Dr Alexandra Leary;
alexandra.leary@gustaveroussy.fr

developed for this poor prognosis population, and immune checkpoint inhibitors (ICIs), are considered the most promising.

Both The Cancer Genome Atlas Research Project and The Proactive Molecular Risk Classifier for EC (ProMisE) classifications identified two EC molecular subgroups that are particularly immunogenic, the mismatch repair-deficient (MMRd)/microsatellite instability-high (MSI-H) and the DNA polymerase epsilon (POLE)-mutant, accounting for 30% and 7% of ECs, respectively.^{4–6} MMR deficiency can arise from germline (Lynch syndrome) or somatic (Lynch-like) mutations in MMR genes (*MLH1*, *MSH2*, *MSH6*, or *PMS2*), or more frequently, from biallelic silencing of the *MLH1* gene due to promoter hypermethylation.⁷ This MMRd/MSI-H subgroup features a high tumor mutation burden (TMB) resulting in a high number of potential neoantigens. Consequently, these tumors exhibit greater CD8⁺ cytotoxic T-cell infiltration compared with their mismatch repair-proficient (MMRp)/non-POLE-mutant counterparts. This immune reactive microenvironment leads to a tumorous adaptive immune resistance, which is defined by the upregulation of immune checkpoint proteins on tumor and immune cells, such as programmed death-ligand 1 (PD-L1), making this EC subgroup an ideal candidate for immunotherapeutic interventions.⁸

Over the last few years, various anti-programmed cell death protein 1 (PD-1) or anti-programmed death-ligand 1 (PD-L1) have shown meaningful clinical activity as a single agent in previously treated advanced or recurrent MMRd/MSI-H EC with overall response rates (ORR) of 40–50% (95% CI, 39.5 to 60.5).^{9–11} Importantly when response to ICI occurs in patients with MMRd EC, its duration is impressive, not reached in KEYNOTE-158 or GARNET with over 40 and 27.6 months follow-up, respectively. Following these results, both agents were approved by the Food and Drug Administration (FDA) and the European Medicines Agency (EMA) for women with advanced or recurrent MSI-H/MMRd EC who have progressed to platinum-based therapy.

The KEYNOTE-775 phase 3 trial demonstrated that the combination of pembrolizumab and lenvatinib in patients progressing post-platinum was statistically and clinically superior to standard chemotherapy in terms of progression-free survival (PFS) and OS in both the MMRp and the all-comer cohorts. On an exploratory analysis, this combination therapy was also found to be effective in the MMRd subgroup, with a confirmed ORR of 41.5% (95% CI, 29.4% to 54.4%).¹² Based on these data, pembrolizumab plus lenvatinib was approved by the FDA for patients with previously treated advanced EC who do not have MSI-H or MMRd tumors, and by the EMA regardless of MMR status.

Recently, four phase 3 randomized clinical trials have demonstrated that the addition of an ICI to carboplatin and paclitaxel and then continued as maintenance therapy, in patients with newly diagnosed advanced or recurrent EC resulted in a statistically and

clinically significant improvement in PFS, particularly in the MMRd/MSI-H subgroup.^{13–16}

To date, MMRd status is considered one of the most robust predictive biomarkers of response to ICI.¹⁷ TMB has also emerged as a candidate biomarker of response to ICI in multiple tumor types, including EC. Most MMRd/MSI-H ECs have high TMB. However, a small subset of MMRd/MSI-H tumors exhibits low TMB (13.5% in the GARNETT trial), and shows a lower ORR of 21%.¹¹ In brief, TMB provides limited predictive value within an MMRd/MSI-H EC population.

A recent publication suggested that clonal, but not subclonal, neoantigen burden predicted response to ICI in patients with MMRd tumors.¹⁸ Finally, the mechanism of MMR deficiency may also be relevant. Two studies have shown that *MLH1* methylation predicted poor outcomes with pembrolizumab.^{19–20} However, this has not been confirmed in larger prospective studies.^{21–22}

As ICIs become the standard of care, there is a growing need for better predictive biomarkers to select patients with MMRd EC unlikely to benefit and uncover potential mechanisms of resistance. A greater understanding of the key differences in the immune contexture of MMRd responders (Rs) versus non-responders (NRs) could inform future trials.

To address this issue, we performed spatial multiplexed immune profiling and clustering analyses to compare the immune tumor microenvironment (iTME) of MMRd EC associated with ICI response (ICI-R) versus ICI non-response (ICI-NR).

METHODS

This was a retrospective, exploratory biomarker-discovery investigation study. All patients included in the study were provided with a specific informative letter, indicating their non-opposition and granting permission for the utilization of archived tumor tissues for research purposes. Additionally, their personal and clinic-pathological data, previously documented in the electronic records of Gustave Roussy Cancer Center, were authorized for use. Anonymization procedures were rigorously implemented to safeguard patient privacy. Prior to commencement, the project underwent thorough scrutiny and received approval from the local Research and Development Committee of Gustave Roussy Cancer Center, ensuring compliance with ethical standards and regulations governing human research.

Case selection and clinical data

A clinically annotated tumor sample cohort of advanced or recurrent MMRd EC from the Gustave Roussy Cancer Center Biobank was established. The inclusion criteria were adult women with histologically proven MMRd EC treated with ICIs between 2016 and 2022, with available tumor samples before ICI treatment. It should be noted that any histological subtype was eligible for the study (eg, endometrioid, serous, clear cell, or mixed).

Patients were classified as ICI-R and ICI-NR, according to the following response criteria, evaluated as per Response Evaluation Criteria in Solid Tumors version 1.1 (RECIST V.1.1): complete response, partial response, or stable disease (SD) for at least 12 months defined ICI-R, whereas progression of disease as the best response or SD for less than 12 months defined ICI-NRs.

Furthermore, a cohort of MMRp EC samples was established and used as a comparator.

Patients' clinicopathological characteristics, treatment, and outcome data were collected from institutional electronic medical records.

Study endpoints

The primary endpoint of the study was to compare the MMRd EC iTME composition in ICI-R versus NR. The iTME evaluation included the following parameters: type of immune cell (IC), density, spatial organization (dispersed or clustered) and localization (intraepithelial, ie,- or stromal, s-), immune co-regulators' expression, and tumor antigen-presenting capacity. All immune biomarkers previously identified were integrated into a cluster analysis to evaluate the heterogeneity of iTME in MMRd EC and to identify combinations of immune features capable of predicting response to ICI.

The secondary objectives include assessing the impact of MMR deficiency mechanisms on iTME, discerning differences in iTME between MMRd and MMRp EC, as well as tracking the evolution of iTME through the disease course and following treatments, with a special focus on exploring immune escape mechanisms.

Immunostaining

Formalin-fixed paraffin-embedded (FFPE) tumor tissue blocks were obtained from the Gustave Roussy Pathology Department. Samples were selected based on the greatest viable tumor cellularity and necrotic samples were excluded. The presence of tumor cells (TCs) in the tumor samples was confirmed by pathological review (CG) of H&E-stained slides.

For immunofluorescence (IF) and chromogen-based immunohistochemistry (IHC) staining, we used the following antibodies: CD3, CD4, CD8, Foxp3, CD20, CD23, CD57, CD68, CD103, CD163, DC-lamp, and cytokeratin, as well as PD-L1, indoleamine 2,3-dioxygenase 1 (IDO-1), T-cell immunoglobulin and mucin containing protein-3 (TIM-3), Lymphocyte activation gene 3 (LAG-3), and human leukocyte antigen class I (HLA-I). Tumor samples from both the MMRd and MMRp EC cohorts were stained sequentially with validated antibody-generating multiplex or monoplex-staining panels (online supplemental materials S1 and S2).

Image collection and analysis

IC subpopulations analyses

For IF IHC panels no. 1–3 and the chromogen-based IHC panel no. 4, the slides were scanned at a high-resolution scanning (20×) using a multispectral imaging system

(Zeiss Axio Scan.Z1). Data from the multispectral camera were accessed by the imaging Visiopharm software. The different IC populations in the intratumoral region of whole-section images were characterized and quantified using cell segmentation and cell phenotype tools. CD8⁺, CD4⁺, Foxp3⁺, and CD20⁺ cells were expressed as the density of cells per mm², whereas CD68⁺, CD163⁺, and DC-lamp⁺ cells were expressed as the percentage of the positive-stained surface.

For chromogen-based IHC panels no. 5 and 6, the slides were scanned at high-resolution scanning (20×) using the Olympus VS120 whole slide scanner. Image analysis was performed using open-source software QuPath V.0.3.0.²³ The different IC populations were characterized and quantified in the intratumoral region of whole-section images using cell detection, and pixel or object classification tools. CD3⁺, CD20⁺, and CD68⁺ cells were expressed as the percentage of positive-stained surface, whereas CD8⁺CD103⁺ cells were expressed as the density of positive cells per mm².

For the evaluation of CD3⁺, CD8⁺, and CD8⁺CD103⁺ T cells, two subpopulations were described within the tumor area: the s- and the, that is, lymphocytes (in direct contact with TCs).

Tumor-infiltrating lymphocytes (TILs) were assessed according to the guidelines described by the International TILs Working Group 2014.²⁴

CD57 marker, included in panel no. 5, allows the identification of two CD57⁺ IC subpopulations: CD57⁺CD3⁻ (natural killer (NK) cells) and CD57⁺CD3⁺ (terminally-differentiated T cells). CD57⁺ ICs were manually quantified and reported as the average density of positive cells per mm² in whole-section images.

Tertiary lymphoid structures assessment

Multiplex chromogenic IHC panel no. 5 and H&E slides were used to evaluate the presence of tertiary lymphoid structures (TLS). TLS was defined as a lymphoid aggregate composed of a central B-cell (CD20⁺) zone with a peripheral T-cell (CD3⁺) zone. Further, a CD23-monoplex IHC panel (panel no. 7) was used to identify follicular dendritic cells within TLSs. TLSs were classified as mature (mature TLS; mTLS) when at least one CD23⁺ IC was detected within them, based on criteria of a previous publication.²⁵ Only mTLS located among TCs and/or within the invasive margin (defined as a fibrous tissue distance of <1 mm from TCs) were included in the analysis.

Immune co-regulators and HLA-I expression analyses

For immune co-regulators and HLA-I chromogen-based IHC panels, slides were scanned at high-resolution scanning (20×) using the Olympus VS120 whole slide scanner.

IDO-1, TIM-3, LAG-3, and PD-L1 expression were manually scored and reported as the average percentage of tumor and ICs with moderate to strong membranous staining in whole-section images. For IDO-1, tumor and IC staining were considered positive when clear cytoplasmic

and/or perinuclear staining was identified. Tonsillar tissue functioned as an external positive control. The percentage of positive s- and ieICs, along with the positive TCs were calculated for each sample. Overall, a tumor sample was considered positive for an immune co-regulator if at least 5% of the cells (IC and/or TC) stained positive. A positivity threshold of 1% was set specifically for assessing the expression of immune co-regulators on ieIC.

HLA-I expression was manually assessed and classified as “retained” or “loss” based on a 10% threshold of TCs in whole-section images, consistent with criteria established in a previous publication.²⁶ Both membranous and cytoplasmic positive staining were considered. Additionally, an H-score was performed (0–300) to quantify the percentage and intensity of the stained TCs (strong: 3+; moderate: 2+; weak: +1; or absent: 0). Normal endometrial glands, stroma, and tumor-associated ICs were used as internal positive controls. Tonsillar tissue was used as the external positive control.

MMR and MLH1 promoter methylation status

MMRd status was diagnosed by IHC and is characterized by the loss of nuclear immunostaining for at least one of the MMR proteins that are routinely examined (MLH1, PMS2, MSH2, and MSH6). Tumors with retained staining for all MMR proteins were designated as MMRp.

The samples were stained sequentially with validated antibody-generating IHC monoplex-staining panels (online supplemental material S3). The MMR IHC panel interpretation was performed by an expert pathologist (CG). Unequivocal nuclear staining of lymphocytes, fibroblasts, or normal epithelium in the vicinity of the tumor served as internal positive control. Tonsillar tissue was used as an external positive control.

Tumors demonstrating either dual MLH1/PMS2 loss or isolated PMS2 were screened for MLH1-promoter methylation using droplet digital PCR (ddPCR; Naica Geode, Stilla). Tumors with confirmed methylation of MLH1 promoter were classified as methylated MLH1 (mMLH1), while tumors with no proven methylation, dual MSH2/MSH6, or MSH6-only loss were defined as non-methylated MMRd (nmMMRd). Subsequently, all nmMMRd EC cases were tested for Lynch syndrome-associated mutations. In our cohort, ddPCR for MLH1 methylation was informative in all except two cases, due to low DNA concentration in the archived FFPE samples.

Clustering analyses

Unsupervised clustering was performed on the MMRd EC cohort using a set of 16 immune biomarkers. This set includes markers for 11 IC subsets, the HLA-I H-score, and the expression of 4 immune co-regulators on ieICs.

A log₂ transformation was applied following the addition of 1 to the immune marker data, and median centering was employed for the normalization of each marker. The Ward 2 algorithm, coupled with Euclidean distance, was used for hierarchical clustering, revealing

subgroups with distinct immune profiles. To enhance heatmap visualization, the expression of each marker was rescaled to the range (–1 to 1), represented by a blue–yellow–red colormap. The corresponding clinico-pathological features, namely MLH1 methylation, mTLS presence, and response to ICI, were displayed at the bottom of the heatmap.

To refine the selection of predictive biomarkers and identify non-redundant subsets for ICI response prediction, we opted for a brute-force feature selection method, motivated by the modest data set size and the manageable computational resource requirements. This approach exhaustively evaluated all possible combinations, ranging from N=2 to N=16 biomarkers, employing the same clustering analysis on the MMRd EC cohort. To assess the significance of individual biomarkers in predicting R versus NR, a Learning Vector Quantization model was employed with five repeats of 10-fold cross-validation.

Through brute-force feature selection, we identified the most predictive immune biomarker subsets as {ieCD8, sCD8, HLA-1, PD-L1}, {ieCD8, sCD8, HLA-1, CD57+T cell}, {ieCD8, sCD8, HLA-1, NK cell}, and {sCD8, HLA-1, CD20, CD68}, all exhibiting three false positives and no false negatives. The top eight predictive biomarkers for Rs versus NRs, as determined by the Learning Vector Quantization model, were ieCD8, PD-L1, LAG-3, IDO-1, CD57+T cell, HLA-1, sCD8, and CD20, ranked in descending order of importance. Considering both the most predictive subsets and the biological relevance of individual markers, we selected the subset {ieCD8, sCD8, HLA-1, PD-L1} for a reduced clustering model. Despite the relatively strong Spearman correlation between ieCD8 and sCD8 ($r=0.84$), excluding either CD8 marker did not yield comparable results.

The identical processing and clustering analysis of the 16 markers were applied to the MMRp EC cohort for immune profiling and subgroup classification. To align the MMRp with the MMRd clusters, both cohorts were processed together, and the same clustering analysis was performed.

Logistic regression analysis

A binomial ridge logistic regression model was trained using the four previously selected markers with R versus NR as the outcome variable. Threefold cross-validation was employed to identify the optimal value of the regularization parameter λ , using binomial deviance as the loss function (mean=0.96, SD=0.24, with best $\lambda=0.02029303$). The area under the receiver operating characteristic curve (AUROC) for the cross-validated samples was 0.92. Subsequently, a final model was refit on the entire data set using the optimal λ . The resulting logistic regression model is described by the following formula: $\text{logit}(p)=1.6274900+1.1239536 \cdot \text{ieCD8}-0.5074075 \cdot \text{sCD8}+1.6437992 \cdot \text{PD-L1}+0.6468771 \cdot \text{HLA-I}$. The analysis was conducted using R V.4.3.2 with the glmnet package V.4.1–8, caret package V.6.0–94, and pROC package V.1.18.5.

Statistical analysis

Statistical analyses were performed for both MMRd and MMRp cohorts. No formal calculation of the power or sample size was performed. Descriptive statistics were used to summarize the clinicopathological characteristics of the patients. Comparisons of categorical variables between subgroups were performed using Fisher's exact test. Comparisons of numerical continuous variables between subgroups were performed using the Mann-Whitney U test. Wilcoxon signed-rank test was used to compare paired samples. Statistical significance was set at $p < 0.05$. Statistical analyses were conducted using GraphPad Prism (V.9.1.2).

PFS and OS estimations were calculated using the Kaplan-Meier method in the MMRd cohort. Subgroup survival comparisons were conducted using the log-rank test. Specifically, survival analyses were performed using R V.4.3.2 with survival package V.3.5–7 and survminer package V.0.4.9.

RESULTS

Study population

29 patients with advanced or recurrent MMRd EC treated with ICIs were identified. For each patient, a pre-ICI recurrent disease sample was preferentially analyzed ($n=11$). If unavailable, a primary tumor sample was included in the analysis ($n=18$) (figure 1A). The main clinicopathological features and treatment details of the patients are summarized in table 1. 20 (69%) patients were classified as ICI-Rs and 9 (31%) as ICI-NRs. There were no imbalances between subgroups in terms of clinicopathological characteristics or previous therapies. Low-grade endometrioid adenocarcinoma was the most common histological subtype in both subgroups. Dual MLH1/PMS2 loss was the most frequent MMR IHC pattern. 22 (81%) MMRd EC cases harbored MLH1 mMLH1 and 5 (19%) were nmMMRd including 3 Lynch syndromes. All nmMMRd cases were ICI-Rs whereas only 64% of mMLH1 were Rs. Most patients in both subgroups received one prior line of platinum-based chemotherapy in the advanced or recurrent setting. Approximately 80% of patients received anti-PD-(L)1 monotherapy, while 20% received combination therapies, all of which were exclusively immune-oncology-based. Radiological response to ICI, as per RECIST V.1.1, is summarized in figure 1A. At the data cut-off of December 2023, with a median follow-up of 35 months, 13 of 20 Rs were still alive with a sustained response to ICI. In contrast, among NRs, only one out of nine patients remained alive. The median PFS was 65 months and 2 months for the R and NR subgroups, respectively (HR 0.14; 95% CI, 0.04 to 0.55; $p < 0.0001$).

Assessment of IC subsets within the TME of MMRd EC and their contribution to ICI response

Both, that is, and s CD8⁺ (cytotoxic) T-cell densities were significantly increased in R versus NR (median ieCD8⁺ T cells: 187.1 cell/mm² vs 2.5 cell/mm², $p=0.0002$;

and median sCD8⁺ T cells: 144.4 cell/mm² vs 4.5 cell/mm², $p=0.03$; figure 1B,C). ICI-R also harbored significantly more CD57⁺CD3⁺ terminally-differentiated T cells (median: 4.1 vs 0.0 cell/mm², $p=0.007$; figure 1B,C). A particular subset of CD8⁺ cells, the CD8⁺CD103⁺ T cells, also known as tumor-resident memory T cells (TRM), showed a trend for higher infiltration in Rs (median: 1.1 vs 0.0 cell/mm², $p=0.08$; figure 1B). There was no significant difference in the overall CD4⁺ T cell, Foxp3⁺CD4⁺ Treg, or CD57⁺CD3⁻ NK cells (figure 1B). Regarding CD20⁺ cell infiltration, the median density was significantly higher in the ICI-R (median: 8.2 cell/mm² vs 1.4 cell/mm², $p=0.03$; figure 1B,C).

Regarding myeloid cells, ICI-R exhibited a significantly higher infiltration of DC-lamp⁺ dendritic cells ($p=0.03$) but no significant differences in M1 or M2 macrophages (online supplemental material S4).

The presence of mTLS is associated with ICI response

In total, 9 (31%) tumor samples of our cohort harbored intraepithelial mTLS and/or within the invasive margin (figure 2A–C), with 8/9 classified as ICI-R (figure 2D). The presence of mTLS was also significantly associated with increased ieCD8⁺ T cells (median: 391.3 cell/mm² vs 61.8 cell/mm², $p=0.0018$).

HLA class I loss may contribute to the lack of ICI efficacy in MMRd EC

Next, we explored the impact of tumor antigen-presenting capacity on ICI efficacy in MMRd EC. Using a cut-off of 10% for HLA-I tumor expression (figure 3A), 28% of samples had HLA-I loss (figure 3B) and harbored drastically lower ieCD8⁺ cell infiltration (median: 4.7 cell/mm² vs 180 cell/mm², $p=0.003$; figure 3C) compared with HLA-I retained tumors. HLA-I loss was significantly associated with a lack of response to ICI (75% NRs vs 14% NRs among the HLA-I retained subgroup, $p=0.04$). Consistent with these results, NRs had a significantly lower median HLA-I H-score compared with Rs (12 vs 152, $p=0.02$).

Immune co-regulator molecules expression of ICI-R versus NR MMRd EC

ICI-Rs were significantly more likely to be PD-L1-positive. Using a cut-off of 5% positive TCs and/or ICs, 80% of ICI-R were PD-L1-positive (vs only 22% of ICI-NR, $p=0.010$). Interestingly, these tumors also expressed other co-inhibitory molecules with 100% of ICI-R being IDO-1-positive (vs 56% of NR, $p=0.005$), 90% being LAG-3-positive (vs 22% of NR, $p=0.0007$), and 90% TIM-3-positive (vs 44% of NR, $p=0.0164$) (figure 4A). Thus ICI-R were more likely to co-express multiple immune co-regulators: 95% of ICI-R expressed two or more co-regulators versus 55% of ICI-NR.

As proximity between TCs and ICs has been suggested as a possible mediator of ICI response, we next focused on the immune co-regulator expression on IC in direct contact with TCs (ieIC). While 89% (8/9) of ICI-NR completely lacked PD-L1 positive ieICs, 67% (6/9) of

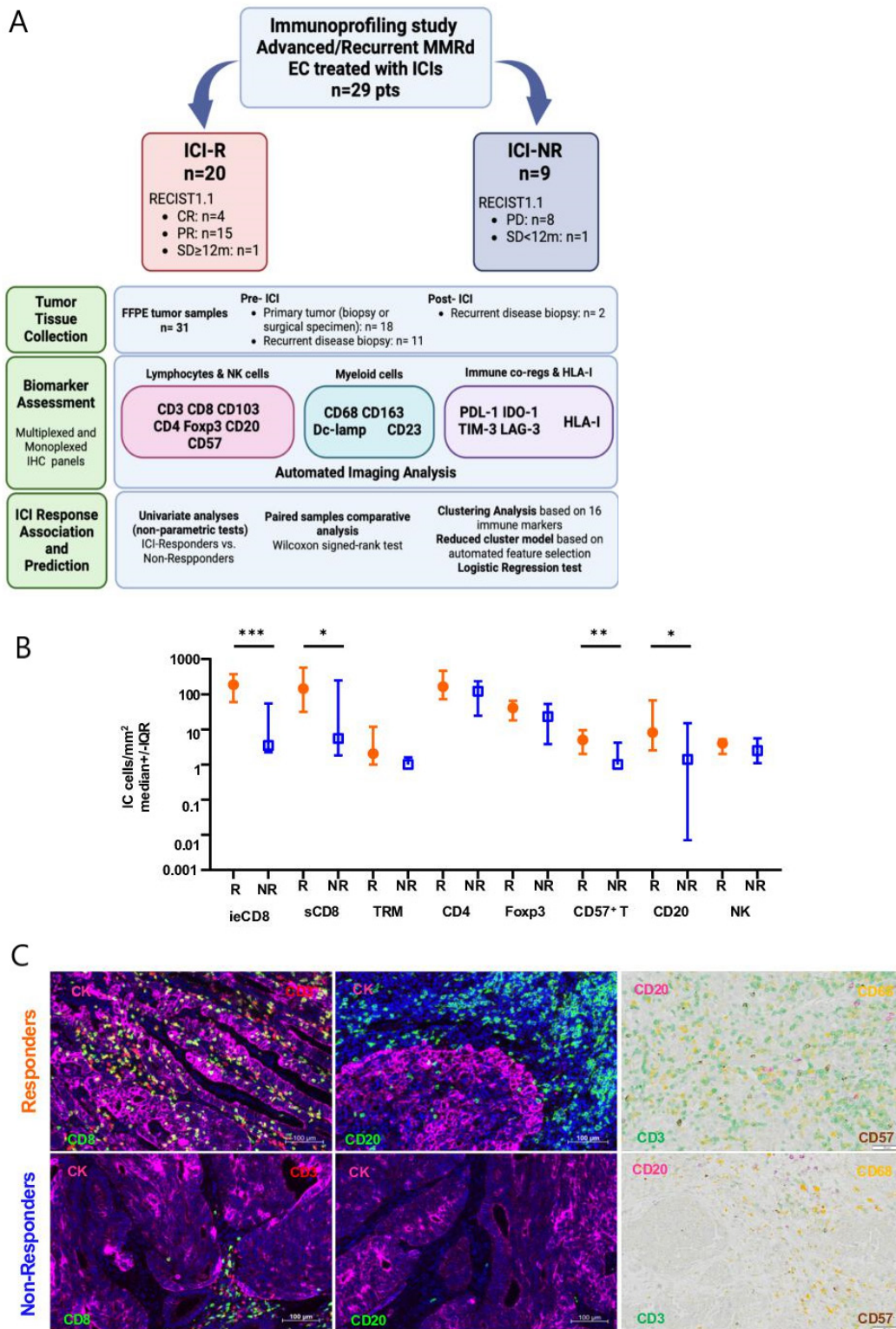


Figure 1 IC subpopulations assessment and their impact on ICI efficacy. (A) Biomarker study overview. (B) Comparative analyses of lymphocyte subsets and NK cell densities expressed as cells per mm^2 between ICI-responders and non-responders, using the Mann-Whitney test. (C) Representative images of panel no. 2 (CD8), no. 3 (CD20), and no. 5 (CD3, CD57) in ICI-responders versus non-responders. CD57+T, terminally differentiated T cell; * p value \leq 0.05; *** p value \leq 0.001. CR, complete response; EC, endometrial cancer; HLA-I, human leukocyte antigen class I; IC, immune cells; ICI, immune checkpoint inhibitor; IDO-1, indoleamine 2,3-dioxygenase 1; Ie, intraepithelial; IHC, immunohistochemistry; LAG-3, lymphocyte activation gene 3; MMRd, mismatch repair-deficient; NK, natural killer; NR, non-responder; PD, progression of disease; PD-L1, programmed death-ligand 1; PR, partial response; R, responder; RECIST 1.1: Response Evaluation Criteria in Solid Tumors version 1.1; S, stromal; SD, stable disease; TIM-3, T-cell immunoglobulin and mucin containing protein-3; TRM, tumor-resident memory T cell.

Table 1 Clinicopathological features and treatment details of the mismatch repair-deficient endometrial cancer cohort

Clinicopathological features	ICI-responders (n=20)	ICI non-responders (n=9)
Age (mean, years)	62	60
Histology (endometrioid/others*)	16 (80%)/4 (20%)	8 (89%)/1 (11%)
Histopathologic grade (low/high)	16 (80%)/4 (20%)	6 (67%)/3 (33%)
MMR IHC pattern	MHL1/PMS2 loss: 16 (80%) MSH2/MSH6 loss: 2 (10%) PMS2 isolated loss: 1 (5%) MSH6 isolated loss: 1 (5%)	MHL1/PMS2 loss: 9 (100%)
MLH1 methylation status	mMLH1: 14 (70%) nmMMRd: 5 (25%) Unknown: 1 (5%)	mMLH1: 8 (89%) nmMMRd: 0 (0%) Unknown: 1 (11%)
FIGO stage (I/II/III/IVA/IVB) at diagnosis	6 (30%)/0 (0%)/9 (45%)/5 (25%)	3 (33%)/2 (23%)/3 (33%)/0 (0%)/1 (11%)
Initial complete surgery	16 (80%)	8 (89%)
Adjuvant radiation therapy/chemotherapy	12 (60%)/6 (30%)	8 (89%)/3 (33%)
Number of prior lines of systemic therapy in the advanced or recurrent setting (n; %)	0L: 2 (10) 1L: 14 (70) 2L: 3 (15) ≥3L: 1 (5)	0L: 1 (11) 1L: 7 (78) 2L: 1 (11)
Prior exposure to platinum in the advanced or recurrent setting	18 (90%)	6 (67%)
ICI regimens	Anti-PD-1 single agent: 10 (50%) Anti-PD-L1 single agent: 5 (25%) Combination†: 5 (25%)	Anti-PD-1 single agent: 7 (78%) Anti-PD-L1 single agent: 1 (11%) Combination‡: 1 (11%)

*Serous carcinoma, clear cell carcinoma, carcinosarcoma, and mixed carcinoma.
 †Anti-PD-1+anti-TIM-3, anti-PD-1+anti-CTLA-4, and anti-PD-1+intratumoral oncolytic virus.
 ‡Anti-PD-1+anti-TIM-3.
 CTLA-4, cytotoxic T-lymphocyte associated protein 4; FIGO, The International Federation of Gynecology and Obstetrics; ICI, immune checkpoint inhibitor; IHC, immunohistochemistry; L, lines; mMLH1, methylated MLH1; nm-MMRd, non-methylated MMRd; PD-L1, programmed death-ligand 1; TIM-3, T-cell immunoglobulin and mucin containing protein-3.

NR tumors harbored positive ieICs for other actionable immune co-regulators, especially IDO-1 and TIM-3 (figure 4B,C). In addition, on analyzing matched pre-ICI and post-ICI samples of two NR patients (patient no. 2 achieved only 6 months of SD and patient no. 5 showed progression as a best response), notable changes in immune co-regulator expression on ieIC were observed. Specifically, there was a remarkable increase in TIM-3 expression in both cases (figure 4D).

The analysis of the immune co-regulator expression on s-ICs and TCs in ICI-Rs versus NRs is summarized in online supplemental material S5.

Impact of MMR deficiency mechanisms on the iTME of EC and its association with ICI efficacy

As stated above, patients with nmMMRd EC in our cohort appeared to respond better to ICIs compared with those with mMLH1 tumors. We then investigated the differences in iTME between mMLH1 and nmMMRd cases. In comparison to their mMLH1 counterparts, nmMMRd EC demonstrated significantly higher levels of ieCD8⁺ (median: 270.6 cells/mm² vs 69.4 cells/mm², p=0.02),

and CD20⁺ (median: 89.7 cells/mm² vs 4.3 cells/mm², p=0.02), as well as higher CD8/Foxp3 ratio (median: 19.0 vs 9.7, p=0.02). nmMMRd tumors also revealed a trend for increased CD4⁺T cell and NK cell densities, as well as a higher CD68/CD163 ratio (online supplemental material S6A, B). nmMMRd cases also demonstrated significant upregulation in most immune co-regulators on ieICs including PD-L1 (median: 15% vs 1%, p=0.03), LAG-3 (median: 20% vs 3%, p=0.01), and TIM-3 (median: 20% vs 5%, p=0.01) (online supplemental material S6C).

The iTME of ICI-NR MMRd may be even more immune-tolerant than MMRp ECs

A cohort of 9 MMRp EC was established using primary tumor (n=5) or metastatic biopsy samples (n=4). Among the MMRp endometrial tumors, the most common histologic subtype was high-grade endometrioid adenocarcinoma, and over half of them had no specific molecular profile (online supplemental material S7).

We next evaluated the iTME of the MMRp EC and compared it to the previously described iTME of NR MMRd tumors. Compared with MMRp EC, NR MMRd

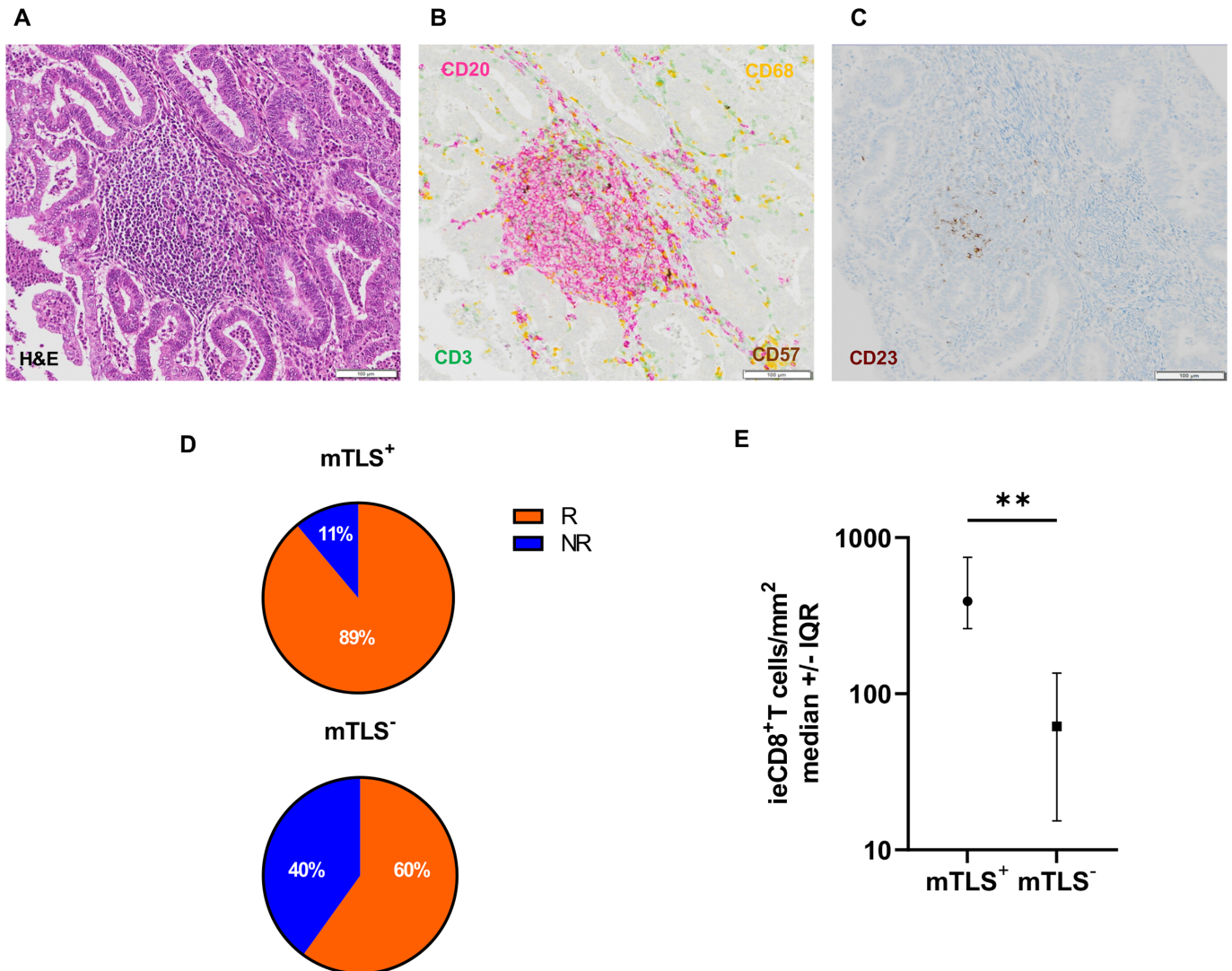


Figure 2 Relevance of mTLS for ICI efficacy. Representative image of an mTLS: (A) H&E, (B) multiplex chromogen-based IHC no. 5, and (C) CD23-monoplex IHC panels. (D) Percentage of ICI-responders and non-responders according to the presence of mTLS. (E) Comparative analysis of ieCD8⁺T cell between mTLS-positive (mTLS⁺) and mTLS-negative (mTLS⁻) tumors, using the Mann-Whitney test. CD3: green, CD20: purple, CD68: yellow, CD57 and CD23: DAB; **p value ≤ 0.01. IC, immune cells; ICI, immune checkpoint inhibitor; ie, intraepithelial; IHC, immunohistochemistry; MP, macrophages; mTLS, mature tertiary lymphoid structures; NR, non-response; R, response.

tumors exhibited significantly decreased ieCD8⁺ T cell (median: 2.5 cell/mm² vs 119 cell/mm², p=0.01), and trend for decreased CD20⁺ cell infiltration (median: 1.4 cell/mm² vs 16.3 cell/mm², p=0.06) (online supplemental material S8A). HLA-I tumor expression was significantly lower among NR MMRd tumors (median H-score: 12 vs 128, p=0.02; online supplemental material S8B). No noticeable differences were detected in the immune co-regulator expression on ieICs (online supplemental material S8C).

Limited impact of pre-ICI standard treatments on iTME evolution

We next investigated the dynamics of iTME of MMRd EC on standard treatments, namely chemotherapy and radiotherapy, prior to ICI initiation. Among the MMRd EC cohort, five patients (three Rs and two NRs) had both

primary tumor and pre-ICI recurrent disease samples. Most of them (4/5) received adjuvant radiotherapy±chemotherapy, and all of them were treated with first-line carboplatin-paclitaxel. Analysis of paired tumor samples revealed no significant changes in CD8⁺, CD4⁺, CD20⁺, or DC-lamp⁺ IC densities, and PD-L1 upregulation on ieIC.

Clustering analysis identified three MMRd EC clusters based on immune biomarkers

The MMRd EC cohort was segregated into three clusters based on 16 immune parameters including 11 IC subsets, HLA-I H-score, and expression of 4 immune co-regulators on ieICs. The three cohorts were characterized by high T-cell infiltrated (high T_{inf}), moderate T-cell infiltrated (intermediate T_{inf}), and desert (figure 5A).

The high T_{inf} cluster accounted for 21% of the entire MMRd EC cohort and was characterized by the highest

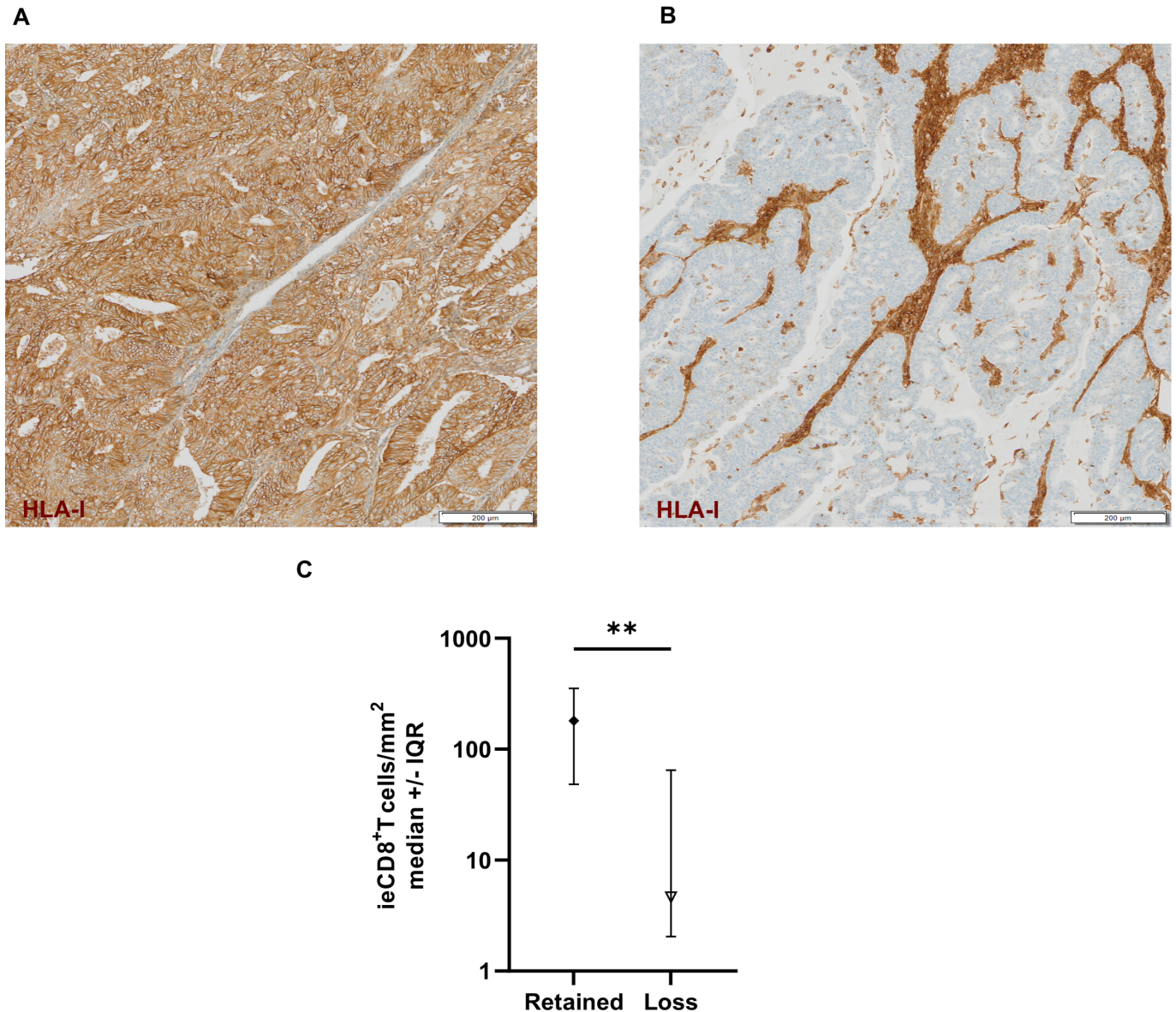


Figure 3 Impact of HLA-I loss on ICI efficacy. Representative images of the HLA-I monoplex immunohistochemistry panel showing two HLA-I tumor expression patterns: (A) HLA-I retained expression and (B) HLA-I loss. (C) Comparative analysis of ieCD8⁺T cell infiltration in HLA-I retained versus loss mismatch repair-deficient endometrial cancer cases (Mann-Whitney test). *p value≤0.05; **p value≤0.01. HLA-I, human leukocyte antigen class; ICI, immune checkpoint inhibitor; NR, non-response; R, response.

CD8⁺ cytotoxic and CD4⁺ helper T-cell infiltration, as well as higher terminally-differentiated CD57⁺ T cell, CD20⁺ cell, and NK cell infiltration. All the tumors in this cluster also had preserved HLA-I and all harbored mTLS. This cluster also showed the highest expression of immune co-regulators. All patients within this cluster were ICI-R (figure 5A).

At the other end of the spectrum, the desert cluster (28% of MMRd cases) exhibited the lowest levels of CD8⁺ cytotoxic, ieTRM, and terminally differentiated CD57⁺ T cells. They were uniformly PD-L1 negative. Seven of the eight tumors included in the desert cluster were ICI-NR (figure 5A).

The predominant subgroup within our cohort was the intermediate T_{inf}, constituting 52% of all MMRd

EC cases. This cluster exhibited moderate infiltration of CD8⁺ cytotoxic and CD4⁺ helper T cells and reduced terminally differentiated CD57⁺ T cells, CD20⁺ cells, and NK cells, compared with the High T_{inf} cluster. Only two cases showed mTLS. Most of the tumors had MLH1 promoter methylation and 87% of cases responded to ICI (figure 5A).

In the clinic, our priority is to develop a predictive assay that is feasible in routine practice and identifies with confidence ICI-NRs to guide these patients toward clinical trials of novel therapies designed to overcome primary resistance. We next aimed to narrow down the selection of parameters from the original data set while maintaining high accuracy in predicting ICI resistance. As detailed in the methods, using a brute-force selection method, a

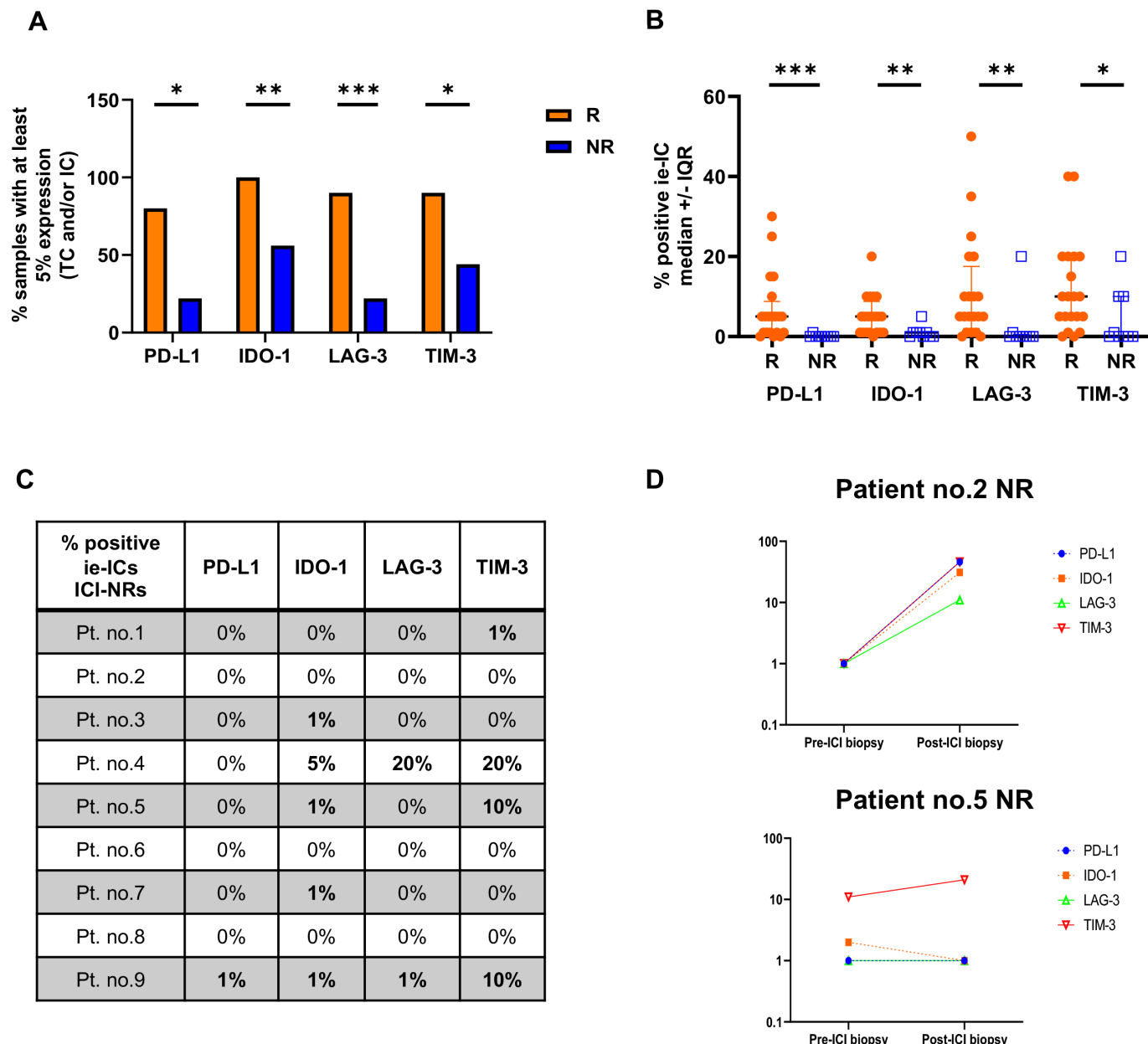


Figure 4 Immune co-regulator expression in ICI-responders versus non-responders. (A) Percentage of samples with $\geq 5\%$ immune co-regulator expression on ICs and/or TCs in ICI-responders versus non-responders. (B) Comparative analysis of immune co-regulator expression on ieICs between ICI-responders versus non-responders using the Mann-Whitney test. (C) Percentage of immune co-regulator positive ieICs in the ICI non-responder subgroup (in bold those reaching 1% positivity cut-off of immune co-regulators' expression on ieICs). (D) Changes in immune co-regulator expression on ieICs in pre-ICI and post-ICI tumor samples from two ICI non-responder cases. *p value ≤ 0.05 ; **p value ≤ 0.01 ; ***p value ≤ 0.001 . IC, immune cell; ICI, immune checkpoint inhibitor; IDO-1, indoleamine 2,3-dioxygenase 1; ie, intraepithelial; LAG-3, lymphocyte activation gene 3; NR, non-responder; PD-L1, programmed death-ligand 1; Pt, patient; R, responder; S, stromal; TC, tumor cell; TIM-3, T-cell immunoglobulin and mucin containing protein-3.

Learning Vector Quantization model was applied to all possible combinations of immune biomarkers and determined a combination of four features as most predictive: ieCD8, sCD8, PD-L1, and HLA-I H-score. This simplified model achieved an overall accuracy of 0.90 in predicting ICI response, identical to that of the 16-marker cluster model. All high T_{inf} tumors were ICI-Rs, whereas approximately 83% of cases in the intermediate T_{inf} cluster responded to ICI. Importantly, the four-marker model

improved the prediction of ICI resistance, where all tumors classified as desert were ICI-NR (figure 5B,C). A logistic regression model using this four-immune marker combination demonstrated excellent discriminative power between ICI-Rs and NRs, with an AUROC of 0.92.

Additionally, these three immune clusters displayed significantly different PFS and OS outcomes (figure 5D). For the high T_{inf} , intermediate T_{inf} , and desert clusters, median PFS durations were 40 months (95% CI, 40 to

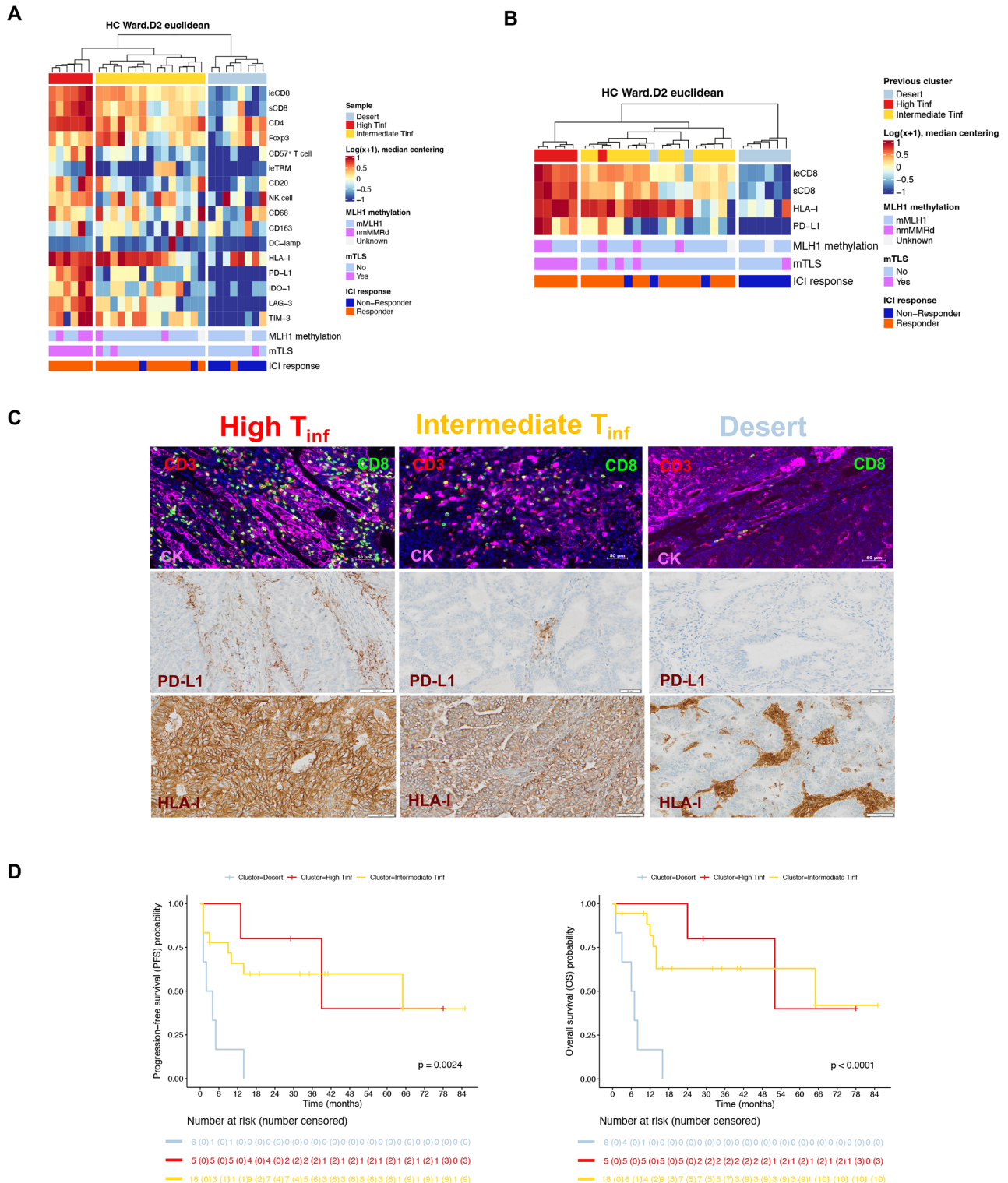


Figure 5 MMRd endometrial cancer immune clusters. (A) Hierarchical unsupervised clustering based on the 16 immune parameters. (B) Cluster model based on four automatically selected immune markers: ieCD8, sCD8, PD-L1, and HLA-I H-score. (C) Images from immunofluorescence panel no. 2 (CD4 and CD8) and chromogen-based immunohistochemistry panel for PD-L1 and HLA-I, illustrating the three immune clusters based on the four-marker model. (D) PFS and OS Kaplan-Meier curves of the three immune clusters based on the four-marker model. ICI, immune checkpoint inhibitor; IDO-1, indoleamine 2,3-dioxygenase 1; ie, intraepithelial; HLA-I, human leukocyte antigen class I; LAG-3, lymphocyte activation gene 3; mMLH1, methylated MLH1; MMRd, mismatch repair-deficient; mTLS, mature tertiary lymphoid structure; NK cell, natural killer cells; nmMMRd, non-methylated MMRd; PD-L1, programmed death-ligand 1; S, stromal; TIM-3, T-cell immunoglobulin and mucin containing protein-3; TRM, tissue-resident memory T-cell.

NA), 65 months (95% CI, 11 to NA), and 3 months (95% CI, 2 to NA), respectively (log-rank *p* value for multigroup comparison, *p*=0.0024). Regarding the median OS, durations were 52 months (95% CI, 52 to NA), 65 months (95% CI, 15 to NA), and 7 months (95% CI, 3 to NA) for the high T_{inf} , intermediate T_{inf} , and desert clusters, respectively (log-rank *p* value for multigroup comparison, *p*<0.0001).

On the other hand, we conducted a cluster analysis of the MMRp EC cohort using the 16-immune marker set. When analyzing MMRd and MMRp cohorts together, we observed that most of the MMRp samples grouped with intermediate T-cell infiltrated or desert MMRd tumors, on the right side of the heatmap. Only three MMRp tumors were part of the high T_{inf} cluster (online supplemental material S9).

DISCUSSION

This exploratory translational research study aimed to address significant knowledge gaps regarding the iTME composition and its influence on ICI efficacy within MMRd EC. Current candidate predictive biomarkers for ICI response primarily hinge on tumor-intrinsic features, namely MMR protein status and TMB, displaying moderate predictive utility. In contrast, our study explored iTME-intrinsic features by combining spatial multiplexed immune profiling and clustering analyses.

On assessment of multiple IC subsets within the TME of the MMRd EC cohort, cytotoxic CD8⁺ TILs, both the, that is, and s subpopulations were most associated with ICI response. Several reports established the prognostic value of CD8⁺ TILs in EC.^{27–28} However, the predictive role of TILs in EC has been scarcely explored. One study showed no significant association between the presence of CD8⁺ ieTILs and response to ICI in MMRd EC.²⁹ These contrasting results may be explained by methodological differences. The previous study used manual counting without details about the number of fields assessed or whether focused on hot spots, whereas we performed automated quantification of the total number of positive TILs per mm² on whole-slide sections.

The present study also identified a rarely described terminally differentiated T-cell subpopulation characterized by the expression of CD57, which was only found within the iTME of ICI responders. This marker identifies a subset of T and NK cells with low proliferative capacity, but increased cytotoxic activity and is associated with better prognosis in multiple tumor types.^{30–31} This T-cell subset, whether present in iTME or the peripheral blood, is also predictive of benefit from ICI in patients with non-small cell lung cancer or urothelial cancer.^{32–33}

The presence of CD8⁺CD103⁺ TRM cells predicts favorable prognosis in multiple tumor types, including EC^{34–35} and response to anti-PD-(L)1 antibodies.³⁴ Here we only found a trend for higher median density of CD8⁺CD103⁺ T cells in ICI-R.

Beyond cytotoxic T cells, our study underscores the substantial role of humoral immunity in the efficacy of ICI as demonstrated by significantly greater levels of CD20⁺ cells and mTLS in ICI-Rs. These findings align with a growing body of evidence suggesting that B cells within the TME support antitumor immunity and promote responses to ICI.³⁶ A previous study demonstrated the positive prognostic impact of mTLS in patients with EC, independent of clinicopathological and molecular factors.³⁷ Moreover, mTLS serves as a significant predictor of response to ICI across multiple solid tumors, regardless of PD-L1 expression. Consistent with our data, the previous study also showed that mTLS-positive tumors displayed higher ieCD8⁺ T-cell density.²⁵

Regarding myeloid cells, we investigated the extent of the antigen-presenting cell involvement in ICI efficacy. Our results suggested a significant increase in DC-lamp⁺ mature dendritic cells in ICI-R tumors. Classical type I HLA molecules are crucial for presenting cellular antigens to T cells and are essential for immunosurveillance and ICI efficacy.³⁸ We found HLA-I loss in 28% of MMRd EC, consistent with a recent publication showing a 21% diffuse loss.²⁶ Importantly, HLA-I loss was associated with significantly lower ieCD8 infiltration and resistance to ICI. In alignment with these findings, various publications have linked the presence of mutations in beta-2 microglobulin, a structural component of major histocompatibility complex-peptide, with the resistance to ICI in the MMRd EC population.^{19–29}

In the context of EC, recent publications have highlighted the prevalence of PD-L1, IDO-1, TIM-3, and LAG-3 expression, being particularly upregulated in the MMRd EC subgroup.^{39–42} We found higher expression of all immune co-regulators in the ICI-R subgroup, both globally and specifically on ieICs, compared with NRs, likely explained by high CD8+Tcell infiltration. PD-L1 expression was not a sine qua non-requirement for a response as 15% of ICI-R lacked PD-L1 expression on ieICs. By comparison, 89% of NRs were PD-L1-negative. When analyzing the predictive utility of PD-L1 upregulation on ieIC, 94% of PD-L1-positive MMRd tumors were responsive to ICI therapy, while 27% of PD-L1-negative tumors were also ICI-Rs. Acknowledging the differences in sample size, response classification, and PD-L1 scoring method (Combined Positive Score), the findings regarding the predictive value of PD-L1 within the MMRd cohort of the GARNET trial appear to be aligned with our data. Indeed, the GARNET trial showed an ORR of 54.9% in MMRd/MSI-H EC with combined positive score (CPS)≥1, compared with 31.3% in those with a CPS<1%. Thus, we contribute to the increasing body of data that PD-L1 expression alone is not sufficient to predict response to ICI within the MMRd EC.

Other co-regulators, particularly TIM-3, and IDO-1, may contribute to primary and acquired immune resistance in patients with MMRd EC. While ICI-NR were almost uniformly PDL1-negative, especially within the tumor compartment, most expressed other actionable

checkpoints, and escape was associated with upregulation in these molecules. Whether targeting immune co-regulators, beyond PD-L1, may overcome immune resistance in a selected subgroup of MMRd EC merits investigation.

Within our study, the MMR loss mechanism appeared relevant for ICI efficacy. All nmMMRd were ICI-R and exhibited significantly greater densities of ieCD8⁺ T cells, CD20⁺ B cells, and a higher CD8/Foxp3 ratio, consistent with a previous study.⁴³ Interestingly, a recent research, based on longitudinal single-cell RNA sequencing of circulating ICs, demonstrated that the mechanism of MMR deficiency may delineate two different modes of response to anti-PD-1 in EC.⁴⁴

As no single immune feature emerged as a robust predictive biomarker, we performed a hierarchical unsupervised clustering analysis of the MMRd EC cohort integrating 16 immune parameters which resulted in three distinct clusters exhibiting striking differences in their immune profiles and response to ICI. Intriguingly, up to 28% of MMRd EC were classified as desert tumors, displaying a poorly infiltrated iTME, with seven of the nine NRs in our cohort included in this cluster. On the other extreme of the immune spectrum, the High T_{inf} cluster, accounting for 21% of MMRd EC, was characterized by a highly inflamed TME, all being ICI-Rs. The most common immune cluster (52%), the intermediate T_{inf} with a moderate T-cell infiltration, exhibited an 87% ICI response.

We streamlined this complex cluster model for hypothetical implementation in clinical use, by automatic feature selection method identifying four key immune parameters: ieCD8, sCD8, PD-L1, and HLA-I H-score. This simplified model recapitulates two crucial factors for ICI efficacy: preserved tumor antigen-presentation capacity and the presence of exhausted cytotoxic T cells. With fewer parameters, it improved the prediction of ICI resistance within the desert cluster (100% were ICI NRs), while slightly adjusting the prediction of ICI sensitivity within the intermediate T_{inf} cluster to 83%. The high T_{inf} cluster consistently identified ICI-Rs with 100% predictive value. Notably, a logistic regression model demonstrated excellent performance of this four-marker combination in distinguishing between ICI-Rs and NRs, with a discriminative power of 92%, outperforming the MMRd status alone. On the other hand, our findings further underscore the prognostic significance of this immune cluster classification.

Furthermore, using archived primary tumor tissue may be deemed acceptable, given our findings suggesting a minimal impact of pre-ICI standard therapies on iTME evolution.

Finally, our study highlighted that ICI-NR MMRd EC harbored a much more immune-tolerant TME than MMRp EC, with drastically lower IC infiltration and antigen-presenting capacity. When both MMRd and MMRp cohorts were integrated in the 16-marker cluster analysis, most MMRp EC segregated within the low T-cell clusters. However, a small subset of MMRp EC exhibited a

high T-cell infiltration, suggesting an increased likelihood of response to ICI. Notably, these findings echo previous studies reporting a high-TIL pattern in 27% and 22% of p53abn and p53 wild-type MMRp EC, respectively.⁴⁵

Limitations of our work include the retrospective nature, the small sample size, the clinical heterogeneity of the study population in terms of treatment line and ICI-based regimens, and the absence of a matched contemporary cohort of patients with MMRd EC who did not receive ICIs in their disease history. This hinders us from providing a methodologically appropriate demonstration of the purely predictive role of the proposed classification. Large-scale prospective randomized studies are warranted to confirm the predictive significance of the biomarkers identified in MMRd EC or other MMRd cancer populations.

To our knowledge, this study represents the first comprehensive comparison of the iTME of MMRd EC ICI-Rs versus NRs. Overall, Rs exhibited significantly greater, that is, and sCD8⁺ and harbored a unique subset of terminally differentiated T cells, together with higher immune co-regulator co-expression. Both high CD20⁺ B-cell infiltration and the presence of mTLS were strongly associated with response to ICI. Furthermore, Rs harbored a highly preserved antigen-presenting capacity as demonstrated by high HLA-I tumor expression and the presence of mature dendritic cells.

No individual immune parameter was powerful enough to discriminate between Rs and NRs. Our clustering analysis suggests that MMRd EC is a heterogeneous immune entity exhibiting at least three distinct immune patterns. We demonstrated that a simplified four-marker model significantly predicted ICI response within MMRd EC. Notably, it identified a desert profile that robustly predicted ICI resistance with a 100% predictive value. Identifying these ICI-resistant patients is vital in clinical practice, as it could steer them towards alternative therapeutic approaches beyond anti-PD-(L1) monotherapies. This simple combination of biomarkers may be useful to select not only patients with MMRd EC but also those with other MMRd cancers, such as colorectal cancer, for clinical trials exploring novel immunotherapeutic approaches.

Author affiliations

¹Gynecological Oncology Programme, Vall d'Hebron Institute of Oncology, Barcelona, Spain

²Gynecological Cancer Translational Research Laboratory, INSERM U981, Gustave Roussy Institute, Villejuif, France

³Laboratoire d'Informatique Paris Descartes (LIPADE), Université Paris Cité, Paris, France

⁴Centre d'Histologie, Imagerie cellulaire et Cytométrie (CHIC), Centre de Recherche des Cordeliers, Centre de Recherche des Cordeliers, Paris, France

⁵Pathology Department, Gustave Roussy Institute, Villejuif, France

⁶Department of Medical Biology and Pathology, Cancer Genetics Laboratory, Gustave Roussy Institute, Villejuif, France

⁷Obstetrics & Gynecology, University of Groningen Faculty of Medical Sciences, Groningen, The Netherlands

⁸Experimental and Translational Pathology Platform (PETRA), AMMICA Inserm US23/UAR CNRS 3655, Gustave Roussy Institute, Villejuif, France

⁹Department of Gynecologic Surgery, Department of Surgery, Gustave Roussy Institute, Villejuif, France

¹⁰Gynecological Cancer Unit, Department of Medical Oncology, Gustave Roussy Institute, Villejuif, France

Contributors AL: Study Guarantor, Conceptualization, Methodology, Formal Analysis, Writing—Original Draft, Visualization, Supervision. JFGB and EYG: Conceptualization, Methodology, Data Collection, Formal Analysis, Writing—Original Draft, Visualization. QZ: Methodology, Formal Analysis, Visualization, Writing—Review and Editing. CG, ER, MdB and CK: Methodology, Formal Analysis, Writing—Original Draft, Visualization, Supervision. ALF, EE, MM and AP: Technical Support, Data Collection, Sample Preparation, Experimentation. SG, AM, PP, JM, and EC-B: Clinical Guidance, Patient Selection, Data Interpretation, Writing—Review and Editing. AO: Data Interpretation, Writing—Review and Editing.

Funding This research was supported by the Comprehensive Program of Cancer Immunotherapy & Immunology I (CAIMI-I) at the Vall d'Hebron Institute of Oncology, funded by the BBVA Foundation (grant 89/2017). Additional support was provided by the Programme Parrainage Chercheur at Institut Gustave Roussy.

Competing interests JFGB reports personal honoraria as speaker from GSK and AstraZeneca; personal fees for travel/accommodation from GSK and AstraZeneca. AL reports institutional funding from AstraZeneca, Clovis, GSK, MSD, Merck Serono, Ability, Zentalis, Agenus, Iovance, Sanofi, Roche, OSEImmuno, BMS, Blueprint; personal fees for consulting or advisory role from Zentalis. JM reports personal fees for consulting or advisory role from Brenus Pharma, GSK, Regeneron; personal fees for travel/accommodation from GSK and MSD; funded research from MSD. EC-B reports personal fees for consulting or advisory role from Ipsen, BMS, Merck, GSK, Sanofi; personal fees for travel/accommodation from Ipsen, BMS, Pfizer. AO reports personal fees for advisory board membership from Agenus, AstraZeneca, Clovis Oncology, Corcept Therapeutics, Dalichi Sankyo, Debiopharm International, Deciphera Pharmaceuticals, Eisai, Exelisis, EMD Serono, F. Hoffmann-La Roche, Genmab, GSK, ImmunoGen, Itheos, Merck Sharps & Dohme de España, SA, Mersana Therapeutics, Myriad Genetics, Novocure, OneXerna Therapeutics, Inc., PharmaMar, Regeneron, Sattucklabs, Seagen, Sutro Biopharma and Zentalis; personal fees for travel/accommodation from AstraZeneca, PharmaMar and Roche; institutional funding from AbbVie Deutschland, Advaxis Inc., Aeterna Zentaris, Amgen, Aprea Therapeutics AB, Bristol Myers Squibb, Clovis Oncology Inc, Eisai limited LTD, F. Hoffmann—La Roche LTD, Immunogen Inc, Merck, Sharp & Dohme de España SA, Millennium Pharmaceuticals Inc, PharmaMar SA, Regeneron Pharmaceuticals and Tesaro Inc.; non-remunerated roles at ESMO (member, Officer, Co-Chair of the ESMO Gynaecological Cancers Congress 2023–2025, Chair of the Gynaecological Track ESMO 2019, Scientific Track Member Gynaecological Cancers ESMO 2018, ESMO 2020, ESMO 2022, member of the Gynaecological Cancers Faculty and Subject Editor for the Gynaecological Clinical Practice Guidelines); a non-remunerated role at GCIG (member and Cervix Cancer Chair on behalf of GEICO); and membership of ASCO, GOG and SEOM.

Patient consent for publication Not applicable.

Ethics approval This study involves human participants and was approved by Scientific Review Committee of Gustave Roussy Cancer Center, Registration Number: 2023-290. The patients have been issued non-opposition informative letters.

Provenance and peer review Not commissioned; externally peer reviewed.

Data availability statement Data are available upon reasonable request. Data sets were generated and/or analysed for this study and are available upon reasonable request.

Supplemental material This content has been supplied by the author(s). It has not been vetted by BMJ Publishing Group Limited (BMJ) and may not have been peer-reviewed. Any opinions or recommendations discussed are solely those of the author(s) and are not endorsed by BMJ. BMJ disclaims all liability and responsibility arising from any reliance placed on the content. Where the content includes any translated material, BMJ does not warrant the accuracy and reliability of the translations (including but not limited to local regulations, clinical guidelines, terminology, drug names and drug dosages), and is not responsible for any error and/or omissions arising from translation and adaptation or otherwise.

Open access This is an open access article distributed in accordance with the Creative Commons Attribution Non Commercial (CC BY-NC 4.0) license, which permits others to distribute, remix, adapt, build upon this work non-commercially, and license their derivative works on different terms, provided the original work is

properly cited, appropriate credit is given, any changes made indicated, and the use is non-commercial. See <http://creativecommons.org/licenses/by-nc/4.0/>.

ORCID iDs

Juan Francisco Grau Bejar <http://orcid.org/0009-0002-3937-4969>

Marco de Bruyn <http://orcid.org/0000-0001-9819-9131>

Ana Oaknin <http://orcid.org/0000-0002-3592-7194>

REFERENCES

- Sung H, Ferlay J, Siegel RL, *et al.* Global cancer statistics 2020: GLOBOCAN estimates of incidence and mortality worldwide for 36 cancers in 185 countries. *CA Cancer J Clin* 2021;71:209–49.
- Siegel RL, Miller KD, Wagle NS, *et al.* Cancer statistics. *CA A Cancer J Clinicians* 2023;73:17–48.
- Oaknin A, Bosse TJ, Creutzberg CL, *et al.* Endometrial cancer: ESMO clinical practice guideline for diagnosis, treatment and follow-up. *Ann Oncol* 2022;33:860–77.
- Kandoth C, Schultz N, Cherniack AD, *et al.* Integrated genomic characterization of endometrial carcinoma. *Nature* 2013;497:67–73.
- Talhouk A, McConechy MK, Leung S, *et al.* Confirmation of promise: a simple, genomics-based clinical classifier for endometrial cancer. *Cancer* 2017;123:802–13.
- Kommos S, McConechy MK, Kommos F, *et al.* Final validation of the promise molecular classifier for endometrial carcinoma in a large population-based case series. *Ann Oncol* 2018;29:1180–8.
- Stelloo E, Jansen AML, Osse EM, *et al.* Practical guidance for mismatch repair-deficiency testing in endometrial cancer. *Ann Oncol* 2017;28:96–102.
- Howitt BE, Shukla SA, Sholl LM, *et al.* Association of polymerase e-mutated and microsatellite-unstable endometrial cancers with neoantigen load, number of tumor-infiltrating lymphocytes, and expression of PD-1 and PD-L1. *JAMA Oncol* 2015;1:1319–23.
- O'Malley DM, Bariani GM, Cassier PA, *et al.* Pembrolizumab in patients with microsatellite instability-high advanced endometrial cancer: results from the KEYNOTE-158 study. *J Clin Oncol* 2022;40:752–61.
- O'Malley D, Bariani GM, Cassier PA, *et al.* 546P pembrolizumab for microsatellite instability-high (MSI-H) or mismatch repair deficient (dMMR) advanced endometrial cancer: long-term follow-up results from KEYNOTE-158. *Ann Oncol* 2022;33:S796–7.
- Oaknin A, Pothuri B, Gilbert L, *et al.* Safety, efficacy, and biomarker analyses of dostarlimab in patients with endometrial cancer: interim results of the phase I GARNET study. *Clin Cancer Res* 2023;29:4564–74.
- Makker V, Colombo N, Casado Herráez A, *et al.* Lenvatinib plus pembrolizumab in previously treated advanced endometrial cancer: updated efficacy and safety from the randomized phase III study 309/KEYNOTE-775. *J Clin Oncol* 2023;41:2904–10.
- Mirza MR, Chase DM, Slomovitz BM, *et al.* Dostarlimab for primary advanced or recurrent endometrial cancer. *N Engl J Med* 2023;388:2145–58.
- Eskander RN, Sill MW, Beffa L, *et al.* Pembrolizumab plus chemotherapy in advanced endometrial cancer. *N Engl J Med* 2023;388:2159–70.
- Colombo N, Harano K, Hudson E, *et al.* LBA40 phase III double-blind randomized placebo controlled trial of atezolizumab in combination with carboplatin and paclitaxel in women with advanced/recurrent endometrial carcinoma. *Ann Oncol* 2023;34:S1281–2.
- Westin SN, Moore K, Chon HS, *et al.* Durvalumab plus carboplatin/paclitaxel followed by maintenance Durvalumab with or without Olaparib as first-line treatment for advanced endometrial cancer: the phase III DUO-E trial. *J Clin Oncol* 2024;42:283–99.
- Marcus L, Lemery SJ, Keegan P, *et al.* FDA approval summary: pembrolizumab for the treatment of microsatellite instability-high solid tumors. *Clin Cancer Res* 2019;25:3753–8.
- Westcott PMK, Muiy F, Hauck H, *et al.* Mismatch repair deficiency is not sufficient to elicit tumor immunogenicity. *Nat Genet* 2023;55:1686–95.
- Bellone S, Roque DM, Siegel ER, *et al.* A phase 2 evaluation of pembrolizumab for recurrent lynch-like versus sporadic endometrial cancers with microsatellite instability. *Cancer* 2022;128:1206–18.
- Borden L, Dvorak J, Barrett Z, *et al.* MLH1 hypermethylation predicts poor outcomes with pembrolizumab in recurrent endometrial cancer (087). *Gynecol Oncol* 2022;166:S59.
- Tinker AV, Sabatier R, Gravina A, *et al.* 2022-RA-1198-ESGO post hoc analysis of objective response rate by mismatch repair protein dimer loss/mutation status in patients with mismatch repair deficient

- endometrial cancer treated with dostarlimab. *Int J Gynecol Cancer* 2022;32.
- 22 Eskander RN, Sill M, Miller A, et al. LBA43 updated response data and analysis of progression free survival by mechanism of mismatch repair loss in endometrial cancer (EC) patients (pts) treated with pembrolizumab plus carboplatin/paclitaxel (CP) as compared to CP plus placebo (PBO) in the NRG GY018 trial. *Ann Oncol* 2023;34:S1284.
 - 23 Bankhead P, Loughrey MB, Fernández JA, et al. Qupath: open source software for digital pathology image analysis. *Sci Rep* 2017;7:16878.
 - 24 Hendry S, Salgado R, Gevaert T, et al. Assessing tumor-infiltrating lymphocytes in solid tumors: a practical review for pathologists and proposal for a standardized method from the international Immunoncology biomarkers working group: part 2: Tils in Melanoma, gastrointestinal tract carcinomas, non-small cell lung carcinoma and Mesothelioma, endometrial and ovarian Carcinomas, squamous cell carcinoma of the head and neck, Genitourinary carcinomas, and primary brain tumors. *Adv Anat Pathol* 2017;24:311–35.
 - 25 Vanhersecke L, Brunet M, Guégan J-P, et al. Mature tertiary lymphoid structures predict immune checkpoint inhibitor efficacy in solid tumors independently of PD-L1 expression. *Nat Cancer* 2021;2:794–802.
 - 26 Friedman LA, Bullock TN, Sloan EA, et al. MHC class I loss in endometrial carcinoma: a potential resistance mechanism to immune checkpoint inhibition. *Mod Pathol* 2021;34:627–36.
 - 27 de Jong RA, Leffers N, Boezen HM, et al. Presence of tumor-infiltrating lymphocytes is an independent prognostic factor in type I and II endometrial cancer. *Gynecol Oncol* 2009;114:105–10.
 - 28 Palomero J, et al. Biomarkers of tumor-reactive CD4+ and CD8+ TILs associate with improved prognosis in endometrial cancer. *J Immunother Cancer* 2022;10:e005443.
 - 29 Konstantinopoulos PA, Luo W, Liu JF, et al. Phase II study of avelumab in patients with mismatch repair deficient and mismatch repair proficient recurrent/persistent endometrial cancer. *J Clin Oncol* 2019;37:2786–94.
 - 30 Zhang S, Liu W, Hu B, et al. Prognostic significance of tumor-infiltrating natural killer cells in solid tumors: a systematic review and meta-analysis. *Front Immunol* 2020;11.
 - 31 Hu G, Wang S. Prognostic role of tumor-infiltrating CD57-positive lymphocytes in solid tumors: a meta-analysis. *Oncotarget* 2018;9:8111–9.
 - 32 Zhou J, Sun W, Zeng X, et al. CD57+CD8+ T cells and response to PD-1/PD-L1 blockade in patients with NSCLC. *JCO* 2023;41:e21189.
 - 33 Fehlings M, Kim L, Guan X, et al. Single-cell analysis reveals clonally expanded tumor-associated CD57+ CD8 T cells are enriched in the periphery of patients with metastatic urothelial cancer responding to PD-L1 blockade. *J Immunother Cancer* 2022;10:e004759.
 - 34 Damei I, Trickovic T, Mami-Chouaib F, et al. Tumor-resident memory T cells as a biomarker of the response to cancer immunotherapy. *Front Immunol* 2023;14:1205984.
 - 35 Workel HH, Komdeur FL, Wouters MCA, et al. CD103 defines intraepithelial CD8+ PD1+ tumour-infiltrating lymphocytes of prognostic significance in endometrial adenocarcinoma. *Eur J Cancer* 2016;60:1–11.
 - 36 Paijens ST, Vledder A, de Bruyn M, et al. Tumor-infiltrating lymphocytes in the immunotherapy era. *Cell Mol Immunol* 2021;18:842–59.
 - 37 Horeweg N, Workel HH, Loiero D, et al. Tertiary lymphoid structures critical for prognosis in endometrial cancer patients. *Nat Commun* 2022;13:1373.
 - 38 Hazini A, Fisher K, Seymour L. Deregulation of HLA-I in cancer and its central importance for immunotherapy. *J Immunother Cancer* 2021;9:e002899.
 - 39 Sloan EA, Ring KL, Willis BC, et al. PD-L1 expression in mismatch repair-deficient endometrial carcinomas, including lynch syndrome-associated and MLH1 promoter hypermethylated tumors. *Am J Surg Pathol* 2017;41:326–33.
 - 40 Mills A, Zadeh S, Sloan E, et al. Indoleamine 2,3-dioxygenase in endometrial cancer: a targetable mechanism of immune resistance in mismatch repair-deficient and intact endometrial carcinomas. *Modern Pathology* 2018;31:1282–90.
 - 41 Moore M, Ring KL, Mills AM. TIM-3 in endometrial carcinomas: an immunotherapeutic target expressed by mismatch repair-deficient and intact cancers. *Modern Pathology* 2019;32:1168–79.
 - 42 Friedman LA, Ring KL, Mills AM. LAG-3 and GAL-3 in endometrial carcinoma: emerging candidates for immunotherapy. *Int J Gynecol Pathol* 2020;39:203–12.
 - 43 Ramchander NC, Ryan NAJ, Walker TDJ, et al. Distinct immunological landscapes characterize inherited and sporadic mismatch repair deficient endometrial cancer. *Front Immunol* 2019;10:3023.
 - 44 Chow RD, Michaels T, Bellone S, et al. Distinct mechanisms of mismatch-repair deficiency delineate two modes of response to anti-PD-1 immunotherapy in endometrial carcinoma. *Cancer Discov* 2023;13:312–31.
 - 45 Talhouk A, Derocher H, Schmidt P, et al. Molecular subtype not immune response drives outcomes in endometrial carcinoma. *Clin Cancer Res* 2019;25:2537–48.